Optical and Thermal Electron Transfer Activation of Dioxygen by Viologen Dithiolene Metalates[⊥]

U. Ammon,[†] C. Chiorboli,[‡] W. Dümler,[†] G. Grampp,[§] F. Scandola,[‡] and H. Kisch*,[†]

Institut für Anorganische Chemie, Universität Erlangen-Nürnberg, Egerlandstrasse 1, D-91058 Erlangen, Germany, Dipartimento di Chimica, Centro di Fotochimica CNR, Universita di Ferrara, I-44100 Ferrara, Italy, and Institut für Physikalische und Theoretische Chemie, Technische Universität Graz, Technikerstrasse 4/I, A-8010 Graz, Austria

Received: April 11, 1996; In Final Form: July 3, 1996[⊗]

Photoinduced electron transfer activation of dioxygen by redoxactive charge-transfer ion pairs of the type $\{A^{2+}[Pt(mnt)_2]^{2-}\}$ (A^{2+} = 2,2′-,4,4′-bipyridinium or cycloalkylated biimidazolium dication; mnt^{2-} = maleonitriledithiolate) occurs through an optical electron transfer within an ion pair. This affords the primary redox products $A^{\bullet+}$ and $[Pt(mnt)_2]^-$ as indicated by laser flash photolysis. Under argon the transients recombine by fast second-order kinetics. Under dioxygen a different behavior is observed. In the case of acceptors with a first reduction potential more positive than −0.6 V back electron transfer prevails. When the potential is more negative however, $A^{\bullet+}$ reduces O_2 by pseudo-first-order kinetics to generate $O_2^{\bullet-}$, while $[Pt(mnt)_2]^-$ accumulates in the solution. Quantum yields increase with decreasing excitation wavelength. This suggests that internal conversion of the initially populated excited state to the photoreactive ion pair charge-transfer state is more efficient upon excitation to the interligand (π,π^*) state (334 nm) than to the metal-to-ligand charge-transfer state (437 or 580 nm). In the latter cases competitive radiationless deactivation *via* metal-centered states occurs. The corresponding Ni and Pd complexes do not exhibit any reactivity due to their very short excited state lifetimes. Formation of $O_2^{\bullet-}$ was proved by ESR spin-trapping techniques. Accumulation of $[Pt(mnt)_2]^-$ occurs also when instead of irradiating, the reaction is performed in the dark at about 160 °C. The activation energy of 108 ± 10 kJ/mol as obtained for the thermal electron transfer from $[Pt(mnt)_2]^{2-}$ to A^{2+} corresponds well to the value calculated from the Hush−Marcus model.

Introduction

The utilization of molecular oxygen for chemical synthesis is a topic of industrial[1] and biological[2] importance. Although dioxygen is a very strong oxidizing agent, many exergonic reactions are kinetically inhibited due to its triplet ground state configuration. With the most common singlet molecules, spin conversion is of very low probability and therefore no reaction occurs. The first electron transfer reduction to generate the superoxide ion can be regarded as the limiting step in dioxygen activation. In principle this step can proceed either thermally or photochemically. Both possibilities are observed in natural and artificial systems. In the respiratory chain of the human organism, cytochrome P450 catalyzes the reduction thermally,[3] while humic acids act as photosensitizers in sun exposed waters.[4] Many nonbiological oxygenations are catalyzed by transition metal complexes.[1] When these reactions occur photochemically, the excited sensitizer, in addition to transferring an electron to O_2, may also catalyze the formation of singlet oxygen. During investigations on the optical electron transfer (ET) within the redoxactive ion-pair-charge-transfer (IPCT) complexes $\{A^{2+}[PtL_2]^{2-}\}$ (A^{2+} = 2,2′- or 4,4′-bipyridinium; L = ethylene-1,2-dithiolate)[5] we observed the fully solvated transients $A^{\bullet+}$ and $[ML_2]^-$, and in some cases a distinct influence of molecular oxygen.

In this article we report a study of the photoinduced ET activation of dioxygen by IPCT complexes between the $[Pt(mnt)_2]^{2-}$ donor and various dicationic viologen and biimidazolium acceptors in DMSO solution (Figure 1). In addition,the activation energy of the thermal ET in the ion pair $\{BQ^{2+}[Pt(mnt)_2]^{2-}\}$ was measured and compared with the value calculated from the Hush−Marcus model.

Experimental Section

Materials. $(NBu_4)_2[M(mnt)_2]$ (M = Ni, Pd, Pt) were prepared according to literature.[6] $(MV)Cl_2$ (Fluka), $(PQ)Br_2$,[7] $(BQ)Br_2$,[7] $(MQ)Br_2$,[8] $(DEDMP)Br_2$,[9] $(P_2BIm)Br_2$,[10] and $(B_2BIm)Br_2$[10] were converted into the corresponding PF_6^- salts by adding to their aqueous solutions a saturated aqueous solution of NH_4PF_6. Spectrograde dimethyl sulfoxide (DMSO) and propylene carbonate (PC) were used without further purification.

Apparatus and Procedures. UV/vis spectra were recorded on a SHIMADZU UV/VIS/NIR-3101PC spectrophotometer using 1 cm cuvettes (Fa. Hellma), which could be evacuated. Oxygen was removed by degassing with ultrasound (about 20 min) under simultaneous bubbling of argon through the solution. Polychromatic irradiations were performed on an optical train with a high-pressure Xe short-arc lamp (XBO 150 W/S) mounted in the lamp-housing O2-A1010 from Photon Technology International Inc. and cutoff filters. To prevent thermal reactions, the cuvettes were water-cooled. Difference spectra were measured in 1 cm tandem cuvettes (Fa. Hellma), by taking the spectra before and after mixing of the isolated solutions. Peroxide tests were carried out with Merckoquant 10011 Peroxide test sticks, which are useful for semiquantitative measurements (sensitivity 0.5 ppm).

Quantum yields were measured with an electronically integrating actinometer (Mülheimer Modell),[11,12] which was calibrated with Aberchrome 540.[13] Intensities at 334, 437, and 580 nm were 2.80×10^{-10}, 9.92×10^{-10}, and 11.44×10^{-10} einstein/s, respectively. The concentration of the donor com-

[†] Universität Erlangen-Nürnberg.
[‡] Universita di Ferrara.
[§] Technische Universität Graz.
[⊥] Dedicated to Professor Waldemar Adam on the occasion of his 60th birthday.
[⊗] Abstract published in *Advance ACS Abstracts,* August 15, 1997.

S1089-5639(97)01880-X CCC: $14.00

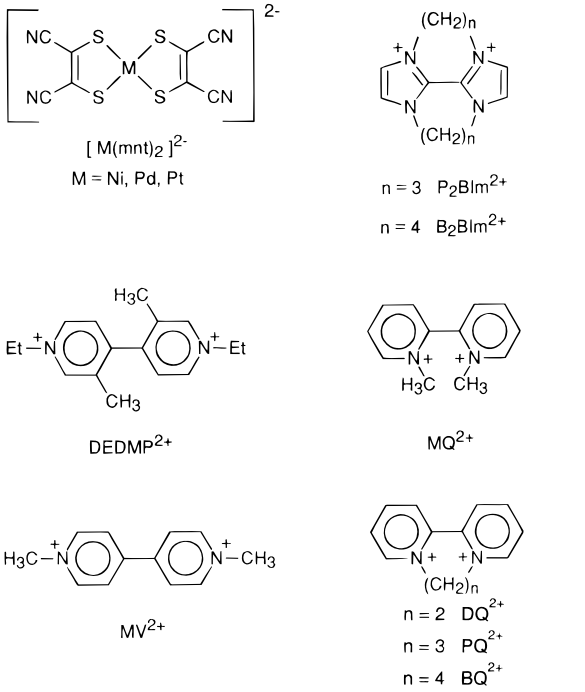

Figure 1. Donor and acceptor components of the ion pairs $\{A^{2+}[M(mnt)_2]^{2-}\}$.

ponent $[Pt(mnt)_2]^{2-}$, applied as NBu_4^+ salt, was 3×10^{-4} M. The acceptor A^{2+} was used as hexafluorophosphate and was present in a 10-fold excess. The reaction was monitored by measuring the concentration of $[Pt(mnt)_2]^-$ through the absorbance at 858 nm ($\epsilon([Pt(mnt)_2]^-) = 12\,190$ L mol^{-1} cm^{-1}). Since the product absorbs at the irradiation wavelength, a quantum yield vs time plot was made for all experiments (eight measurements with a time interval of 2000 s). The initial quantum yield was then obtained by extrapolation to $t = 0$. The quantum yields listed in Table 4 are mean values of three measurements with a deviation smaller than 20%.

ESR measurements were made with a JEOL-PE-3X X-band ESR-Spectrometer with 100 kHz field modulation. The magnetic field strength and the microwave frequency were measured by means of a DRUSCH-RMN 2 type gaussmeter and a microwave frequency counter, type hp-5245. Irradiations were performed inside the ESR-cavity with an Osram HBO 500W/2 high-pressure mercury lamp attached to a water IR filter of 20 cm length.

Laser flash photolysis was performed as reported[14] with a J&K frequency-doubling ruby laser ($\lambda_{exc} = 347$ nm, pulse width = 25 ns, energy = 100 mJ), a monochromator (Applied Photophysics), and a photomultiplier (Hamamatsu 928) as a detection system. The amount of the absorbed laser light was obtained with an actinometric method based on benzophenone triplet absorption. Initial concentrations were 1.33×10^{-4} M (donor) and 3.33×10^{-3} M (acceptor). Absorbance at 347 nm was always higher than 2. The acceptor radical cations were detected at 400 nm ($MV^{\bullet+}$) and 380 nm ($BQ^{\bullet+}$, $MQ^{\bullet+}$, $P_2BIm^{\bullet+}$). $[Pt(mnt)_2]^-$ was detected at 830 and 840 nm. The rate constant k_{-2} for the bimolecular back electron transfer was obtained by a $1/A$ vs time plot of the transient signal. The observed slope k_{obs} was multiplied by the absorptivity to obtain k_{-1}. Absorptivities of the acceptor radical cations were measured in MeCN through spectroelectrochemistry.[15] In the case of $BQ^{\bullet+}$ and $MQ^{\bullet+}$, a dimerization prevented a direct determination and only approximate absorptivities were obtained. It was estimated that only 10% are present as monomers;[15] therefore the measured values ($\epsilon_{380}(MQ^{\bullet+}) = 600$ M^{-1} cm^{-1}; $\epsilon_{380}(BQ^{\bullet+}) = 1280$ M^{-1} cm^{-1}) were multiplied by the factor 10 in the case of $BQ^{\bullet+}$ and $MQ^{\bullet+}$. The rate constant k_1 for the reduction of dioxygen by the acceptor radical cation (pseudo first order because of the excess of dioxygen) resulted directly from the slope of a ln(A) *vs* time plot.

Blank experiments to unravel the consecutive reaction of the superoxide anion were performed in the dark and under illumination ($\lambda > 570$ nm) by adding a 66-fold excess of KO_2 or H_2O_2 (as 30% aqueous solution) to a solution (DMSO or propylene carbonate) of the donor ($[Pt(mnt)_2]^{n-}$; $n = 1, 2$) or the acceptor (MQ^{2+}). Superoxide scavenging experiments were conducted by illuminating solutions of $(NBu_4)_2[Pt(mnt)_2]$ (1×10^{-4} M) and $MQ(PF_6)_2$ (1×10^{-3} M) in DMSO in presence of a 10- and 100-fold excess (relative to the donor) of benzyl or benzoic anhydride.

Kinetic experiments of the thermal ET (E_a) were performed in a light-protected thermostat (Haake F 3-S; 40−250 °C ± 0.01 °C). Air-saturated propylene carbonate solutions were heated in the dark to different temperatures (25, 50, 75, 100, 124, 148, 159, 172, and 182 °C), and the concentration of the monoanion was (through its absorbance at 858 nm) measured at different times (0, 20, 40, 60, and 80 min). From the initial slopes of a ln(c/c_0) *vs* time plot the rate constants k_{obs} were obtained at different temperatures. Division of k_{obs} by $K_a[A^{2+}]$ afforded the k_{et} values ($[A^{2+}] = 3 \times 10^{-3}$ M; $K_a = 70$ M^{-1} as calculated from the Eigen−Fuoss equation assuming an ionic strength of 0.01 M). E_a was determined from the slope of a ln(k) *vs* $1/T$ plot. No formation of $[Pt(mnt)_2]^-$ occurs when $(NBu_4)_2[Pt(mnt)_2]$ is employed under identical experimental conditions.

Results and Discussion

IPCT complexes of type $\{A^{2+}[Pt(mnt)_2]^{2-}\}$ exhibit optical ET from $[Pt(mnt)_2]^{2-}$ to A^{2+}.[16] Recently we showed by laser flash photolysis[5] that under nitrogen the transient redox products recombine by a fast second-order reaction. Under oxygen a different behavior is observed, depending on the reduction potential of the acceptor. In the case of MV^{2+} and PQ^{2+} it is more positive than −0.6 V (in CH_3CN *vs* SCE) and the same kinetics as under nitrogen is found, while the acceptors BQ^{2+}, MQ^{2+} and P_2BIm^{2+} [17] have more negative potentials and behave differently.

Laser excitation ($\lambda_{exc} = 347$ nm) of a DMSO solution of $\{MQ[Pt(mnt)_2]\}$ generated from 3.33×10^{-3} M $MQ(PF_6)_2$ and 1.33×10^{-4} M $(NBu_4)_2[Pt(mnt)_2]$ afforded $MQ^{\bullet+}$ and $[Pt(mnt)_2]^-$.[5] Figure 2a shows the absorbance decay of $MQ^{\bullet+}$ monitored at 380 nm in argon-(1) and oxygen-saturated solutions (2). Under argon the rather long-lived transient ($t_{1/2} = 1.87 \times 10^{-5}$ s) decays by a second -order rate law ($k_{-1}(MQ^{\bullet+}) = 5.5 \times 10^9$ M^{-1} s^{-1}), representing the nearly diffusion-controlled back electron transfer (Figure 2b). Under oxygen a very fast first-order decay is observed ($t_{1/2} = 5.5 \times 10^{-7}$ s) (Figure 2c). $[Pt(mnt)_2]^-$, which was monitored at 830 nm (Figure 2d), behaves similarly to $MQ^{\bullet+}$ in argon-saturated solutions (curve 1 in Figure 2d), while it decayed much slower under oxygen (curve 2 in Figure 2d). In this case, the transient could be also observed on the millisecond time scale and the decay did not follow first or second-order kinetics.

Table 1 summarizes the behavior of complexes with four different acceptors. In the case of MV^{2+}, the presence of oxygen does not change the kinetics and a second-order decay of the transients is observed. The rate constant of $k_{-1}(MV^{\bullet+}) = (6.0 \pm 1) \times 10^9$ M^{-1} s^{-1} is in the same order of magnitude as reported in a previous paper[5] for other acceptors and is close to the diffusion-controlled value. When the acceptor potential is

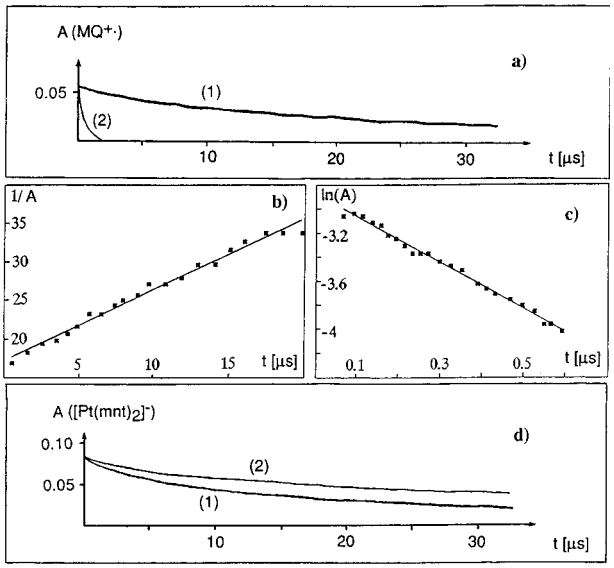

Figure 2. Laser flash photolysis ($\lambda_{exc} = 347$ nm) of {MQ[Pt(mnt)$_2$]} generated from $MQ(PF_6)_2$ (3.33×10^{-3} M) and $(NBu_4)_2[Pt(mnt)_2]$ (1.33×10^{-4} M). (a) Decay of $MQ^{\bullet+}$ ($\lambda_{obs} = 380$ nm), in (1) argon- and (2) oxygen-saturated DMSO. (b) $1/A$ vs t plot of $MQ^{\bullet+}$ in argon saturated DMSO. (c) $\ln(A)$ vs t plot of $MQ^{\bullet+}$ in oxygen -saturated DMSO. (d) Decay of $[Pt(mnt)_2]^-$ ($\lambda_{obs} = 830$ nm), in (1) argon- and (2) oxygen-saturated DMSO.

more negative than -0.6 V, the second-order decay of $A^{\bullet+}$ under argon ($k_{-1}(BQ^{\bullet+}) = 2.2 \times 10^{10}$ s^{-1} M^{-1}; $k_{-1}(P_2BIm^{\bullet+}) = 3.4 \times 10^{10}$ s^{-1} M^{-1}) becomes first order under oxygen ($k_2'(BQ^{\bullet+}) = 1.26 \times 10^6$ s^{-1}; $k_2'(MQ^{\bullet+}) = 1.92 \times 10^6$ s^{-1}; $k_2'(P_2BIm^{\bullet+}) = 4.72 \times 10^6$ s^{-1}). At the same time $[Pt(mnt)_2]^-$ is accumulated.

These observations are in accord with a primary optical ET step (eq 1) followed by a secondary ET to dioxygen (pseudo first order since the concentration of dioxygen in solution (0.0021 M)[19] is 2 orders of magnitude higher than that of $A^{\bullet+}$) (eq 3). Simultaneously the diffusion-controlled back electron transfer (eq 2) occurs. The latter seems to be highly favored over oxygen reduction ($E_{1/2}(O_2/O_2^-)$ in DMSO is -0.74 V *vs* SCE[20]) in the case of MV^{2+} ($E_{1/2}$ ($MV^{2+/\bullet+}$ in DMSO is -0.46 V *vs* SCE[19]). From the known rate constant of this process (eq 3) in acidic DMSO[19] ($k_2 = 2.3 \times 10^{-5}$ M^{-1} s^{-1}) and the solubility of dioxygen in DMSO, it is calculated that the rate of back electron transfer under the given experimental conditions ($c[Pt(mnt)_2]^- = 6.72 \times 10^{-6}$ M) is at least 400 times larger than the rate of O_2^- formation. For the reactive acceptor MQ^{2+} a similar estimation reveals that now superoxide formation is favored 24 times over back electron transfer.

$$\{A^{2+}[Pt(mnt)_2]^{2-}\} \xrightarrow{h\nu} A^{\bullet+} + [Pt(mnt)_2]^- \quad (1)$$

$$A^{\bullet+} + [Pt(mnt)_2]^- \xrightarrow{k_{-1}} A^{2+} + [Pt(mnt)_2]^{2-} \quad (2)$$

$$A^{\bullet+} + O_2 \xrightarrow{k_2} A^{2+} + O_2^- \quad (3)$$

While the rate constants k_{-1} are all in the range of diffusion control and do not significantly depend on the acceptor potential, the rate constants of dioxygen reduction k_2 decrease with more positive potential (see Table 2). This is depicted in Figure 3 for the corresponding pseudo-first-order rate constants, indicating that in the case of $MV^{\bullet+}$ the value of k_2' drops below that of k_{-1}'.

The same reactions as observed in flash photolysis occurred also in continuous irradiation experiments. Figure 4 contains

TABLE 1: Relation between Reduction Potential of Acceptor A^{2+} and Reaction Order of the Decay of the Transients $A^{\bullet+}$ and $[Pt(mnt)_2]^-$ Generated in DMSO under Argon and Oxygen by Laser Flash Photolysis at $\lambda_{exc} = 347$ nm

	MV-[Pt(mnt)$_2$]	BQ-[Pt(mnt)$_2$]	MQ-[Pt(mnt)$_2$]	P_2BIm-[Pt(mnt)$_2$]
$E_{1/2}(A^{2+/+})^a$	-0.45[18]	-0.67[18]	-0.76[16]	-1.12[10]
$A^{\bullet+}$, Ar (O_2)	2 (2)	2 (1)	2 (1)	2 (1)
$[Pt(mnt)_2]^-$, Ar (O_2)	2 (2)	2[b]	2[b]	2[b]

[a] In CH_3CN *vs* SCE. [b] Accumulation of $[Pt(mnt)_2]^-$.

TABLE 2: Rate Constants for ET Reactions of $A^{\bullet+}$ to $[Pt(mnt)_2]^-$ (k_{-1}, k_{-1}') and O_2 (k_2, k_2')

	$E_{1/2}$ (V vs SCE)	k_2 (M^{-1} s^{-1}) (=$k_2'/[O_2]$)	k_{-1} (M^{-1} s^{-1})	k_2' (s^{-1})	k_{-1}' (s^{-1}) (=$k_{-1}x[Pt^-]$)[a]
MV^+	-0.45	2.3×10^5[b]	6.0×10^9	4.8×10^2	4.0×10^4
BQ^+	-0.67	6.0×10^8	2.2×10^{10}	1.3×10^6	1.5×10^5
MQ^+	-0.76	9.1×10^8	5.5×10^9	1.9×10^6	3.7×10^4
P_2BIm^+	-1.12	2.2×10^9	3.4×10^{10}	4.7×10^6	2.3×10^5

[a] $[Pt^-] = c([Pt(mnt)_2]^-$. [b] From ref 19.

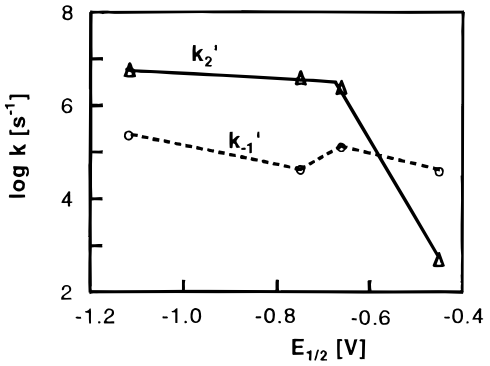

Figure 3. Dependence of the pseudo-first-order rate constants for the ET reactions of $A^{\bullet+}$ to $[Pt(mnt)_2]^-$ (k_{-1}') and O_2 (k_2') on the reduction potential of the bipyridinium acceptor.

the spectrum obtained during irradiation of {MQ[Pt(mnt)$_2$]} at $\lambda > 570$ nm in air-saturated DMSO. The increase of absorbance at 400 nm and the appearance of an isosbestic point at 578 nm and a new band at 870 nm ((π,π^*)-transition of $[Pt(mnt)_2]^-$) indicated the clean oxidation of the dianion (Figure 4a). At longer irradiation times, the band of $[Pt(mnt)_2]^-$ disappeared and a new absorption at 395 nm was observed (Figure 4a(i)). Irradiation experiments at $\lambda > 400$ nm exhibited the same spectral changes, with the exception that a subsequent photoreaction was observed. The absorption band at 395 nm disappeared at the expense of a new band with a maximum at 457 nm (Figure 4b).

Two isosbestic points at 423 and 480 nm pointed to a clean reaction (vide infra). Formation of the monoanion was also observed upon irradiation at $\lambda > 645$ nm, wavelengths at which absorption by the IPCT complex is nine to ten times higher than that of its separated components. This suggests that the photoreactive state has IPCT character. BQ^{2+} and P_2BIm^{2+} exhibited the same behavior while MV^{2+} induced no change of the absorption spectrum (Table 3). $DEDMP^{2+}$ ($E_{1/2} = -0.84$ V) and B_2BIm^{2+} ($E_{1/2} = -1.39$ V), which were not investigated by flash photolysis experiment, are also reactive while PQ^{2+} ($E_{1/2} = -0.56$ V) is not. These results are in good agreement with the time-resolved experiments indicating that dioxygen activation occurs only when the potential of the acceptor is more negative than about -0.6 V. In no case was accumulation of $[Pt(mnt)_2]^-$ observed when Pt was replaced by Ni or Pd.

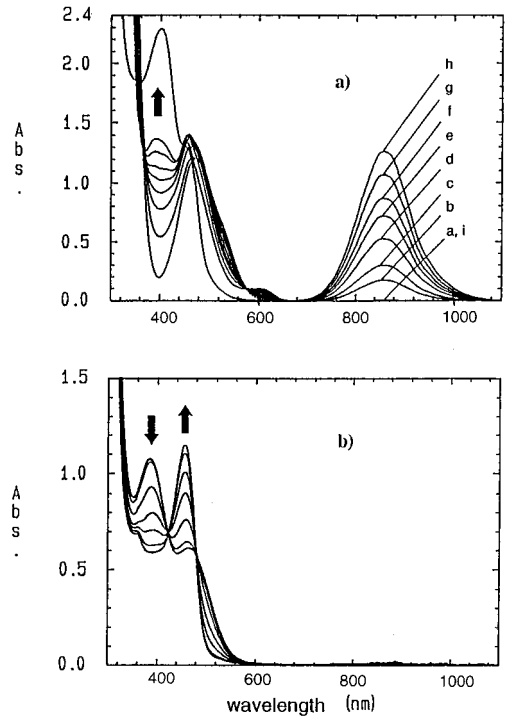

Figure 4. Spectral changes during irradiation of {MQ[Pt(mnt)$_2$]} generated from 4.2×10^{-4} M $(NBu_4)_2[Pt(mnt)_2]$ and 3.6×10^{-3} M $MQ(PF_6)_2$ in air-saturated DMSO. (a) Experiment at $\lambda > 570$ nm, $t =$ 0 (a), 6 (b), 15 (c), 25 (d), 36 (e), 49 (f), 71 (g), 111 (h), and 300 (i) min. (b) Experiment at $\lambda \geq 400$ nm, $t = 6-50$ min.

TABLE 3: Dependence of the Formation of $[Pt(mnt)_2]^-$ on the Acceptor Potential upon Irradiating $\{A^{2+}[Pt(mnt)_2]^{2-}\}$ in Air-Saturated Solutions at $\lambda > 570$ nm (Potentials in V *vs* SCE)

	MV^{2+}	PQ^{2+}	BQ^{2+}	MQ^{2+}	$DEDMP^{2+}$	P_2BIm^{2+}	B_2BIm^{2+}
$E_{1/2}(A^{2+/+})$	−0.45	−0.56	−0.67	−0.76	−0.84	−1.12	−1.39
reactivity	−	−	+	+	+	+	+

The fact that no reaction was observed when the corresponding nickel or palladium complexes were irradiated can be related to the nature of the lowest excited state. In $(NBu_4)_2[M(mnt)_2]$ (M = Ni, Pd), no excited states were detected on the nanosecond time scale[21,22] while the lifetime of $*[Pt(mnt)_2]^{2-}$ was estimated as >10 ns.[21] Figure 5 contains the spectra measured before and after mixing of $MQ(PF_6)_2$ and $(NBu_4)_2[M(mnt)_2]$ (M = Ni, Pd, Pt) solutions. The solid lines represent the spectra of the separate components (A^{2+} and $[ML_2]^{2-}$), while the dashed lines indicate the additional IPCT bands that are more clearly seen in the corresponding difference spectra (insets of Figure 5). From the position of the LF band relative to the IPCT band one can conclude that radiationless deactivation *via* the LF state (either singlet or triplet) as compared to ET from the IPCT state should be more efficient for M = Ni, Pd than for M = Pt.

Quantum yields of $[Pt(mnt)_2]^-$ formation were measured in propylene carbonate by monitoring the absorbance at 858 nm. Table 4 displays the values in the case of two different IPCT complexes at three different wavelengths (334, 437, and 580 nm); an increase of the quantum yield with decreasing irradiation wavelength was observed. This resembles the photooxidation of $(NBu_4)_2[M(mnt)_2]$ (M = Ni, Pd, Pt) in halocarbon solvents.[23] It was proposed that ET may be fast enough to occur from vibrationally excited CTTS states.[24,25] This is in accord with the observation that also the nickel complex underwent photooxidation,[23] although $*[Ni(mnt)_2]^{2-}$ is very short-lived. In the IPCT complexes reported here, ET occurs most likely from the lowest excited (and vibrationally relaxed) state and the wavelength dependence of ϕ can be rationalized as follows. From the absorption spectrum of {MQ[Pt(mnt)$_2$]} one can estimate that the minima of the potential energy surfaces of the IL(π,π^*), MLCT, LF, and IPCT states are located at 315 (380), 206 (580), 160 (750), and 152 (785) kJ/mol (nm), respectively. When the corresponding potential energy curves are drawn as a function of the Pt−S bond length, the minimum of the IPCT state should be slightly displaced to the left as compared to the ground state (Figure 6), since partial oxidation of $[Pt(mnt)_2]^{2-}$ shortens the Pt−S bond.[26] In the case of the other states, M−S antibonding orbitals are involved[26−28] and the minima are displaced to the right of the ground state, an effect that should be strongest for the flat potential curve of the LF state. Irradiation at 334 and 437 nm (Figure 6, arrow 1) populates the IL state at high and the MLCT state at low vibrational levels. After relaxation, internal conversion to the IPCT state may be equally favored. However, since the MLCT state is much closer in energy to the LF state than the IL state, competitive population of the LF state should occur and the reactive IPCT state becomes less populated. This effect should be stronger upon excitation at 580 nm (Figure 6, arrow 2) at which wavelength both the LF and IPCT states are populated.

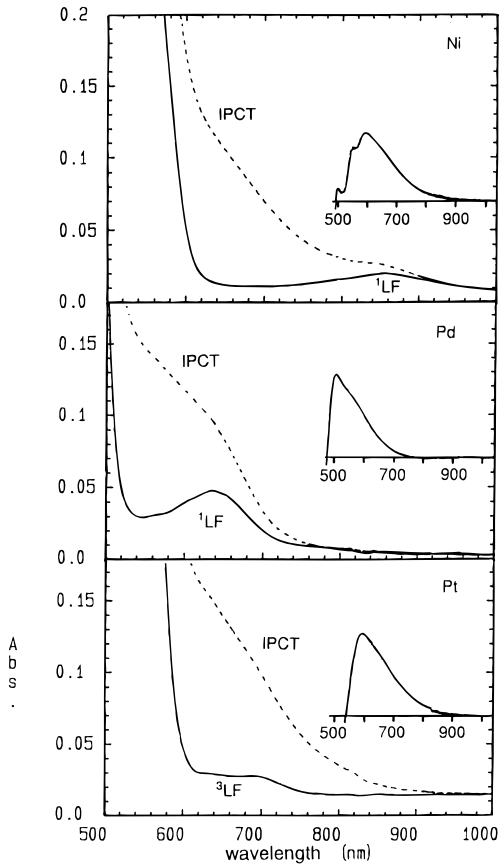

Figure 5. Absorption spectra of $MQ(PF_6)_2$ (1.9×10^{-2} M) and $(NBu_4)_2$-$[M(mnt)_2]$ (1.3×10^{-3} M) (M = Ni, Pd, Pt) in DMSO/THF (1/4, v/v), measured in tandem cuvettes before (—) and after (- - -) mixing; the insets show the corresponding difference spectra.

TABLE 4: Quantum Yield of $[Pt(mnt)_2]^-$ Formation as a Function of Wavelength and Acceptor

	ϕ_{334}	ϕ_{437}	ϕ_{580}
$BQ^{2+}[Pt(mnt)_2]^{2-}$	0.060	0.034	0.024
$MQ^{2+}[Pt(mnt)_2]^{2-}$	0.029	0.015	0.010

Different from the photooxidation[23] of $(NBu_4)_2[Pt(mnt)_2]$, no correlation is found between the reduction potential of the acceptor and the quantum yield. On the contrary, the acceptor BQ^{2+}, which is less reducing, induces a 2-fold higher quantum

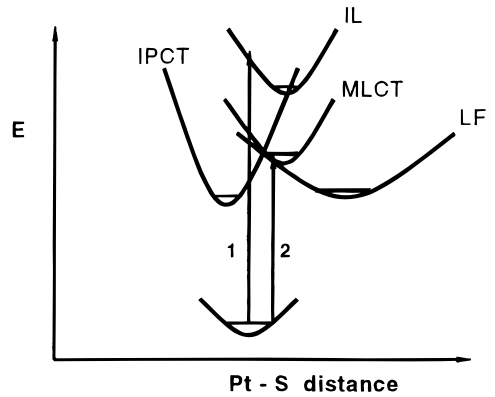

Figure 6. Potential energy curves of ground and lowest excited states of {MQ[Pt(mnt)$_2$]} as a function of the Pt−S bond length.

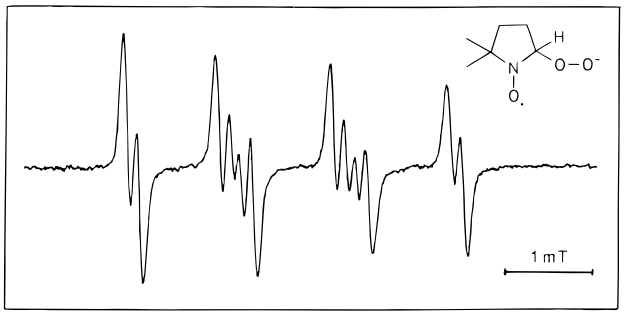

Figure 7. ESR spectrum of DMPO−O_2^- obtained by illumination of {MQ[Pt(mnt)$_2$]} generated from (NBu$_4$)$_2$[Pt(mnt)$_2$] (4.4×10^{-3} M) and MQ(PF$_6$)$_2$ (0.1 M) in the presence of DMPO in air-saturated propylene carbonate ($\lambda > 570$ nm).

yield than $MQ^{2.+}$ This is astonishing since $BQ^{\bullet+}$ reacts slower with O_2, and thus the unproductive back electron transfer, which decreases the quantum yield, should become more important. From the fact that the quantum yield of product formation is about two times larger for the poorer acceptor BQ^{2+}, one can conclude that the rate of the secondary ET step (eq 3) is not the limiting factor. This seems to be rather the primary optical ET (eq 1), the efficiency of which is given by the product of $F_{IP}\eta_{et}\eta_{ce}$, wherein the first term describes the fraction of contact ion pair present, and the two following terms are the efficiencies of optical ET and cage escape, respectively.[5] Since overlap of the donor and acceptor π-systems is a prerequisite for ET, the different acceptor geometries may be decisive. It is known that the ideal, sandwichlike geometry of the two planar components of {MV[Pt(mnt)$_2$]} is changed to a less favorable chainlike arrangement when the nonplanar BQ^{2+} is introduced.[29,30] This should be more pronounced in the case of the MQ^{2+} acceptor since the twist angle increases when the reduction potential becomes more negative.[32] Accordingly, diminished overlap may decrease the efficiency of optical ET and therefore induce a lower quantum yield.

To obtain unequivocal evidence for the intermediate superoxide ion, irradiation was performed in the presence of the spin-trap 5,5-dimethyl-1-pyrroline-*N*-oxide (DMPO)[34] in the cavity of an ESR-spectrometer. The expected spin adduct is rather long-lived according to its half-life of 80 s in H_2O at pH = 6.[35] Figure 7 shows the ESR spectrum of the DMPO−O_2^- spin adduct generated by illumination of a solution of {MQ[Pt(mnt)$_2$]} in air-saturated propylene carbonate at $\lambda > 570$ nm in presence of DMPO. The obtained coupling constants of a_N = 12.9 G, $a_{H\beta}$= 10.4 G, and $a_{H\gamma}$ = 1.4 G agree very well with published values (a_N = 12.9 G, $a_{H\beta}$= 10.2 G, $a_{H\gamma}$ = 1.5 G).[36]

In the presence of other reactive acceptors (B_2BIm^{2+}, P_2BIm^{2+}, BQ^{2+}), identical ESR spectra were obtained, while

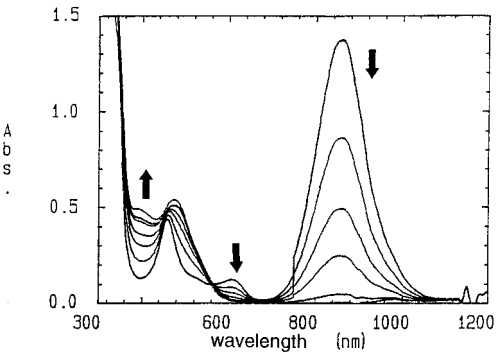

Figure 8. Reaction spectrum during irradiation ($\lambda > 570$ nm) of (NBu$_4$)[Pt(mnt)$_2$] (1.2×10^{-4} M) and H_2O_2 (8.0×10^{-1} M) in DMSO.

no signal was observable in the case of unreactive acceptors, NBu_4^+ salts, analogous nickel complexes, or a blank experiment with DMPO as single component. No evidence was found for a spin adduct of singlet oxygen and DMPO (nine lines, a_N = 7.0 G, $a_H\gamma$ = 3.5 G[37]). This is in accord with experiments employing the $^1O_2$-quencher DABCO (diazabicyclo[2.2.2]-octane). No inhibition of the photoreaction was observed, and a mechanism involving formation of $^1O_2$ and its reduction by $A^{\bullet+}$ can be excluded.

Several consecutive reactions of the superoxide anion may occur in the illuminated solution. No unequivocal evidence for oxidation of the solvent DMSO to dimethylsulfone and for a nucleophilic attack under formation of a fluorescent pyridone[38] was obtained. In a blank experiment it was found that KO_2 reduces $[Pt(mnt)_2]^-$ to $[Pt(mnt)_2]^{2-}$ and O_2. However this pathway would prevent accumulation of $[Pt(mnt)_2]^-$ and is therefore of minor importance. The main reaction seems to be disproportionation of $HO_2^\bullet$, formed by protonation of $O_2^{\bullet-}$, to H_2O_2 and O_2. However, all attempts to detect H_2O_2 in the reaction failed. This suggested that it may have reacted further with one of the components present in the solution. Although MQ(PF$_6$)$_2$ reacted with H_2O_2, the observed changes of the absorption spectrum did not correlate with the changes occurring in the short-wavelength region upon longer irradiation (Figure 4a). When (NBu$_4$)$_2$[Pt(mnt)$_2$] was treated with H_2O_2 thermally or photochemically, oxidation to the monoanion took place. However, when (NBu$_4$)[Pt(mnt)$_2$] was used in the same type of experiment, the changes in the absorption spectrum were the same as in the long time irradiation of the authentic system. This photoreaction was about 10 times faster than the thermal reaction at room temperature (Figures 8 and 4a).

We therefore assume that upon prolonged irradiation at $\lambda >$ 570 nm complete decomposition of the dithiolene generates the free (*Z*)-mnt^{2-} ligand[39] (λ_{max} = 390 nm in DMSO). Higher energetic excitations afford a subsequent (*Z*)-(*E*)-isomerization of the free ligand and are responsible for the spectral changes depicted in Figure 3b. Efforts to scavenge O_2^- by competition reactions with benzyl or benzoic anhydride[40] were not successful.

Recently we have shown that the relation between optical and thermal ET within these ion pairs can be analyzed in terms of the Hush−Marcus model.[16,41−43] For {BQ[Pt(mnt)$_2$]} the activation energy of thermal ET was calculated as 117 kJ/mol from optical and thermodynamic data.[16] This suggests that the photoinduced ET activation of O_2 may occur also thermally at sufficient high temperatures (eq 4).

$$A^{2+} + D^{2-} \underset{k_{-1}}{\overset{k_1}{\rightleftharpoons}} A^{\bullet+} + D^{\bullet-} \xrightarrow[k_2]{O_2} A^{2+} + O_2^- + D^{\bullet-} \quad (4)$$

Thus, air-saturated and strictly light-protected propylene carbon-

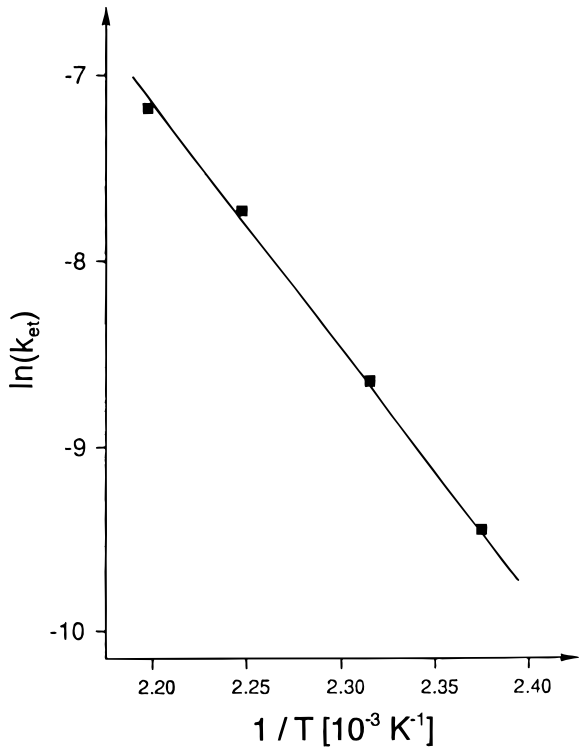

Figure 9. Arrhenius plot of rate constants of thermal electron transfer.

ate solutions of {BQ[Pt(mnt)$_2$]} were heated, and the concentration of the monoanion was measured at different reaction times. In kinetic terms, reaction 4 represents a chain of equilibrium reactions (eq 5, $BQ^{2+} = A^{2+}$; $[Pt(mnt)_2]^{2-} = D^{2-}$) followed by an irreversible bimolecular reaction (eq 3).

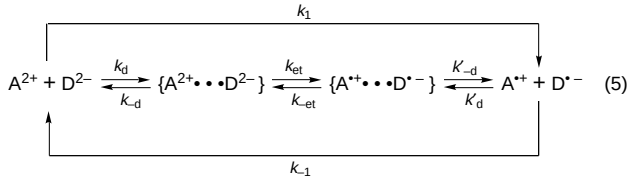

(5)

To obtain the rate constant of the thermal ET, some simplifications were made. In a previous paper k_{et} of {PQ[Pt(mnt)$_2$]} was calculated as 2×10^{-3} s^{-1}.[16] Since k_{et} in {BQ[Pt(mnt)$_2$]} should be even smaller, due to the higher redox potential difference, this step should be much slower than diffusion out of the solvent cage (k'_{-d} and K_d' are in the range of 10^8 s^{-1} and 10^{10} M^{-1} s^{-1}, respectively). Contrary to that, back electron transfer should be much faster than formation of $\{A^{2+} + D^{2-}\}$.[44] Thus eq 5 can be simplified to eq 6.

$$A^{2+} + D^{2-} \underset{k_{-d}}{\overset{k_d}{\rightleftharpoons}} \{A^{2+}\cdots D^{2-}\} \underset{k'_d}{\overset{k_{et}}{\rightleftharpoons}} A^{\bullet+} + D^{\bullet-} \qquad (6)$$

Assuming steady-state conditions for the intermediates and equal concentrations of $A^{\bullet+}$ and $D^{\bullet-}$ at the early stage of the reaction, the rate of O_2^- formation is only dependent on the concentration of the donor (eq 7, $K_a = k_d/k_{-d}$).[46,47]

$$d[O_2^-]/dt = k_{et}K_a[A^{2+}][D^{2-}] = k_{obs}[D^{2-}] \qquad (7)$$

Since the rate of superoxide ion formation corresponds to the accumulation of $D^{\bullet-}$, the reaction can also be expressed as the disappearance of D^{2-} (eq 8). Integration leads to eq 9.

$$-\frac{d[D^{2-}]}{dt} = k_{obs}[D^{2-}] \qquad (8)$$

$$\ln\frac{[D^{2-}]}{[D^{2-}]_0} = -k_{obs}t \qquad (9)$$

Thus a plot of $\ln([D^{2-}]/[D^{2-}]_0)$ *vs* t leads to a straight line at short (0−1200 s) reaction times. Deviations at longer time are due to partial decomposition. From k_{obs}' as obtained from the slope, the following values of k_{et} were calculated according to eq 7: 8×10^{-5}, 1.8×10^{-4}, 4.5×10^{-4}, and 7.7×10^{-4} s^{-1} for 148, 159, 172, and 182 °C.

Figure 9 displays the corresponding Arrhenius diagram. From the resulting straight line (correlation coefficient = 0.9993), an activation energy of 108 ± 10 kJ/mol is obtained. This is in excellent agreement with the value of 117 kJ/mol[16] calculated recently.

References and Notes

(1) Lopez, L. *Top. Curr. Chem.* **1990**, *156*, 117.
(2) Martell, A. E.; Sawyer, D. T. *Oxygen Complexes and Oxygen Activation by Transition Metals*; Plenum Press: New York and London, 1988; p 131.
(3) Guengerich, F. P.; Mac Donald, T. L. *Acc. Chem. Res.* **1984**, *17*, 9.
(4) Wagnerova, D. M.; Lang, K.; Stopka, P.; Damerau, W. *J. Photochem. Photobiol. A.* **1992**, *67*, 187.
(5) Kisch, H.; Dümler, W.; Chiorboli, C.; Scandola, F.; Salbeck J.; Daub, J. *J. Phys. Chem.* **1992**, *96*, 10323.
(6) Davison, A.; Holm, R. H. *Inorg. Synth.* **1967**, *10*, 8.
(7) Homer, R. F.; Tomlinson, T. E. *J. Chem. Soc.* **1960**, 2498.
(8) Ebbesen, T. W.; Ferraudi, G. *J. Phys. Chem.* **1983**, *87*, 3712.
(9) Stoehr, C.; Wagner, M. *J. Prakt. Chem.* **1893**, *48*, 1.
(10) Thummel, R. P.; Goulle, V.; Chen, B. *J. Org. Chem.* **1989**, *54*, 3057.
(11) Amrein, J.; Gloor, J.; Schaffner, K. *Chimia* **1974**, *28*, 185.
(12) Zeug, N.; Bücheler, J.; Kisch, H. *J. Am. Chem. Soc.* **1985**, *107*, 1459.
(13) Heller, H. G.; Langan, J. R. *J. Chem. Soc., Perkin Trans 2* **1981**, *71*, 341.
(14) Chiorboli, C; Scandola, F.; Kisch, H. *J. Phys. Chem.* **1986**, *90*, 2211.
(15) Salbeck, J.; Kisch, H. Unpublished results.
(16) Dümler, W.; Kisch, H. *New. J. Chem.* **1991**, *15*, 649.
(17) Lemke, M.; Knoch, F.; Salbeck, J.; Kisch, H. *Chem. Ber.* **1995**, *128*, 131.
(18) Nunn, I.; Eisen, B.; Benedix, R. Kisch, H. *Inorg. Chem.* **1994**, *33*, 5079.
(19) Andrieux, C. P.; Hapiot, P.; Saveant, J. H. *J. Electroanal. Chem.* **1985**, *189*, 121.
(20) Sawyer, D. T.; Roberts, J. L., Jr. *J. Electroanal. Chem.* **1966**, *12*, 90.
(21) Persaud, L.; Sharma, D. K.; Langford, C. H. *Inorg. Chim. Acta* **1986**, *114*, L5.
(22) Lindsay, E.; Malkhasian, A. Y. S.; Langford, C. H. *Inorg. Chem.* **1994**, *33*, 944.
(23) Vogler, A.; Kunkely, H. *Inorg. Chem.* **1982**, *21*, 1172.
(24) Shirom, M.; Weiss, M. *J. Chem. Phys.* **1972**, *56*, 3170.
(25) Shirom, M.; Siderer, Y. *J. Chem. Phys.* **1972**, *58*, 1250.
(26) Alvarez, S.; Vicente, R.; Hoffmann, R. *J. Am. Chem. Soc.* **1985**, *107*, 6253.
(27) Mc Cleverty, J. A. *Prog. Inorg. Chem.* **1968**, *10*, 49.
(28) Shupack, S. I.; Billig, E.; Clark, R. J. H.; Williams, R; Gray, H. B. *J. Am. Chem. Soc.* **1964**, *86*, 4594.
(29) Ammon, U.; Knoch, F.; Kisch, H. *Z. Kristallogr.* **1995**, *210*, 78.
(30) As known from the solid state structure of BQ[Ni(mnt)$_2$].[31]
(31) Knoch, F.; Schmauch, G.; Kisch, H. *Z. Kristallogr.* **1995**, *210*, 76.
(32) Angles of 20, 50, and 64° have been reported for DQ^{2+},[33a] PQ^{2+},[33b] and BQ^{2+},[31] respectively (See Figure 1).
(33) (a) Willner, I.; Ayalon, A.; Rabinovitz, M., *New. J. Chem.* **1990**, *14*, 685. (b) Knoch, F.; Schmauch, G.; Kisch, H. *Z. Kristallogr.* **1995**, *210*, 225.
(34) Harbour, J. R.; Bolton, J. R. *Biochem. Biophys. Res. Commun.* **1975**, *64*, 803.

(35) Buettner, G. R.; Oberley, L. W. *Biochem. Biophys. Res. Commun.* **1978**, *83*, 69.
(36) Buettner, G. R. *Free Radical Biol. Med.* **1987**, *3*, 259.
(37) Ben-Hur, E.; Carmichael, A.; Riesz, P.; Rosenthal, I. *Int. J. Radiat. Biol.* **1985**, *48*, 837.
(38) Nanni, E. J., Angelis, C. T.; Dickson, J.; Sawyer, D. T. *J. Am. Chem. Soc.* **1981**, *103*, 4268.
(39) Fernandez, A.; Kisch, H. *Chem. Ber.* **1984**, *117*, 3102.
(40) Sawyer, D. T.; Stamp, J. J.; Menton, K. A. *J. Org. Chem.* **1983**, *48*, 3733.
(41) Hush, N. S. *Prog. Inorg. Chem.* **1967**, *8*, 391.
(42) Curtis, J. L.; Sullivan, B. P.; Meyer, T. J. *Inorg. Chem.* **1980**, *19*, 3833.
(43) Kisch, H. *Coord. Chem. Rev.* **1993**, *125*, 155.
(44) Application of the Hush−Marcus model afforded values of 10^{11}−10^{13} M^{-1} s^{-1} for the {PQ[Pt(mnt)$_2$]} system.[45]
(45) Dümler, W. Ph.D. Thesis, University of Erlangen-Nürnberg, **1989**.
(46) Wilkins, R. G. *Kinetics and Mechanism of Reactions of Transition Metal Complexes*; VCH Weinheim: New York, 1991.
(47) Benson, S. W. *The Foundations of Chemical Kinetics*; Mc Graw-Hill: New York, 1960.